



The major influence of anterior and equatorial zonular fibres on the far-to-near accommodation revealed by a 3D pre-stressed model of the anterior eye

Yutian Pu^a, Ziyuan Liu^b, Lin Ye^c, Yunxin Xia^a, Xiaoyong Chen^b, Kehao Wang^{a,*}, Barbara K. Pierscionek^c

^a Key Laboratory for Biomechanics and Mechanobiology of Ministry for Education, Beijing Advanced Innovation Center for Biomedical Engineering, School of Engineering Medicine and School of Biological Science and Medical Engineering, Beihang University, Beijing, China

^b Department of Ophthalmology, Beijing Key Laboratory of Restoration of Damaged Ocular Nerve, Peking University Third Hospital, Beijing, China

^c Faculty of Health, Education, Medicine and Social Care, Medical Technology Research Centre, Anglia Ruskin University, Bishops Hall Lane, Chelmsford, United Kingdom

ARTICLE INFO

Keywords:

Zonules
Accommodation
Lens
Finite element model
Ocular biomechanics

ABSTRACT

Purpose: To explore the synergistic function of the ligaments in eye, the zonular fibres, that mediate change in eye lens shape to allow for focussing over different distances.

Methods: A set of 3D Finite Element models of the anterior eye together with a custom developed pre-stress modelling approach was proposed to simulate vision for distant objects (the unaccommodated state) to vision for near objects (accommodation). One of the five zonular groups was cut off in sequence creating five models with different zonular arrangements, the contribution of each zonular group was analysed by comparing results of each specific zonular-cut model with those from the all-zonules model in terms of lens shape and zonular tensions.

Results: In the all-zonular model, the anterior and equatorial zonules carry the highest tensions. In the anterior zonular-cut model, the equatorial zonular tension increases while the posterior zonular tension decreases, resulting in an increase in the change in Central Optical Power (COP). In the equatorial zonular-cut model, both the anterior and posterior zonular tensions increase, causing a decreasing change in COP. The change in COP decreases only slightly in the other models. For vitreous zonular-cut models, little change was seen in either the zonular tension or the change in COP.

Conclusions: The anterior and the equatorial zonular fibres have the major influence on the change in lens optical power, with the anterior zonules having a negative effect and the equatorial zonules contributing a positive effect. The contribution to variations in optical power by the equatorial zonules is much larger than by the posterior zonules.

1. Introduction

Accommodation is a complex opto-biomechanical process in the eye which describes the change in eye lens shape to allow for the eye to focus on objects over a wide range of distances. This function is active in eyes below the sixth decade of life and gradually decreases with age; the age-related loss of accommodative function is called presbyopia.

The mechanism of accommodation involves ciliary muscle: a ring of smooth muscle located within the eye, the contraction and relaxation of which causes the lens to change shape [1]. The zonular system consists

of several different groups of suspensory ligaments that connect the lens equatorial region and different parts of the ciliary muscle. By contracting and relaxing, the ciliary muscle alters the tension in the zonular fibres, and this leads to a change the lens surface curvatures and thickness and thereby the refractive power to meet visual demands. The synergistic functional mechanism of different zonular groups is closely related to how the lens shape changes during the process of accommodation.

The prerequisite for analysing the synergistic actions of different groups of suspensory ligaments during the accommodative process is a deep understanding of the physiological functions of the zonular system.

* Corresponding author.

E-mail address: kehaowang@buaa.edu.cn (K. Wang).

<https://doi.org/10.1016/j.cmpb.2023.107815>

Received 31 May 2023; Received in revised form 9 September 2023; Accepted 14 September 2023

Available online 15 September 2023

0169-2607/© 2023 Elsevier B.V. All rights reserved.

Most of the zonular fibres originate from the posterior flat part of the ciliary body (pars plana) and traverse anteriorly to firm attachment to the surface of the ciliary process [2,3] where they are divided into three major groups, namely the anterior, the posterior, and the equatorial zonular fibres. These three groups of zonular fibres are inserted into the lens capsule, a semi-elastic basement membrane within which envelops the lens, with the majority inserted in the peripheries of the anterior and posterior surfaces and the rest inserted in the equatorial region [1–3]. Other structures, including the vitreous zonule and anterior hyaloid membrane, have been purported to modulate lens shape change under the contraction and relaxation of the ciliary muscle [4–6].

Current accommodative theories differ in their explanation of the role of the different groups of zonular fibres, the synergetic behaviour of different zonular groups and the interactions between these groups with anterior hyaloid membrane and lens capsule in the process of accommodation. The classical “relaxation theory” proposed by Helmholtz, postulates that different groups of zonular fibres have synchronous tensional behaviour when stretching the lens to a relatively flattened, unaccommodated state for distance vision and they decrease their tensions collectively to allow the lens to return to a more spherical shape in the accommodative state [7,8]. The major theory that challenges the Helmholtzian theory was proposed by Schachar who suggested that the anterior and posterior parts of the zonular fibres behave differently from the equatorial zonule during accommodation: the latter is under tension during the process of accommodation, whilst the anterior and posterior zonules relax [9,10]. Support from the vitreous in the accommodative process was proposed by Coleman who stated that contraction of the ciliary muscle induces a pressure difference between the anterior aqueous humour and the posterior vitreous body thereby causing a forward movement of the lens [11]. The gradient distribution of this pressure difference was theorised to produce a steeper central curvature and a flatter peripheral curvature of the anterior lens surface in order to increase the ocular refractive power [11].

The iris blocks the view of the lens equatorial region where the zonule is located when examining the eye using optical imaging methods and the low contrast and poor resolution of the images obtained from ultrasound or MRI measurements render it difficult to examine the *in vivo* functions of these critical structures involved in the accommodative process [12,13]. Computational modelling serves as a powerful substitute to explore questions that cannot be fully understood through *in vivo* or *in vitro* approaches.

Most previous models have considered near to far accommodation by stretching the lens from a relatively spherical shape into a more flattened shape [14–18]. Burd et al. [14] firstly demonstrated the necessity in considering geometrical nonlinearity during Finite Element (FE) simulations; their lens models, which were applied with equatorial stretching forces, demonstrate support for the Helmholtzian theory. Schachar and Bax [15] stretched their lens models using different combinations of three major groups of zonular fibres and demonstrated the importance of zonular settings on the deformation and optical performance of the lens models. Hermans et al. [16] further considered different inserting regions of zonular fibres on the lens capsule using axisymmetric models although they found that this factor does not play an important role in accommodation. Wang et al. [17,18] considered the influence of a broader range of model parameters and, provided the three major groups of zonules with ability to move in different directions, a better physiological correlation can be provided by altering the zonular angles. The lens has a complex optical system attributed to the fact that it has a gradient distribution of refractive index which increases from the periphery to the central nuclear region where it remains relatively constant [19]. Such a gradient index distribution is determined by the distribution and local concentrations of the structural proteins of the lens, the crystallins and this may further influence the biomechanical properties [19]. Further models developed by the same group [20] included a gradient distribution of elastic moduli for the lens to consider the opto-mechanical interactions, of which a comprehensive

understanding is still needed. These above-mentioned models have applied tension to the zonular fibres to deform the lens from an accommodated state to an unaccommodated state. Yet, the opposite process *i.e.*, modelling from the unaccommodated, flatter lens to the accommodative state, is required to properly understand the role of the zonule.

The far-to-near accommodation had not been modelled until recent years because modelling the deformation of the lens from a stressed state to a less stressed state requires applying pre-stretch or pre-stress to the model. Wilkes et al. [21] accomplished such a process by creating a temperature field and applying it to the zonule with a hypothetical thermal expansion that stretched the lens into the unaccommodated state before the formal simulation. Cabeza et al. [22] introduced initial capsular stress to the lens model in the unaccommodated state so that the lens could return to the accommodative state when the zonular tension was released. The roles of different muscle fibres were considered by Knaus et al. who developed a model driven by the action of the ciliary muscle [23]; this model mainly focused on analysing functions of ciliary muscle fibres in different directions and therefore adopted a relatively simpler arrangements of the zonular fibres [23].

Functions of the zonular fibres have been explored by *in vitro* mechanical stretching to analyse their material properties [24,25], and by modelling studies to consider their macro or individual functions [26, 27]. The supporting effect of the lens by the vitreous has also been considered by Ljubimova et al. [28] who included the vitreous in their models and captured the influence of the vitreous body, namely the so-called “squeezing” effect.

The present study aims to explore the synergistic function of different zonular groups using three-dimensional finite element models of the anterior eye together with a custom developed pre-stress modelling approach. The developed model can be used to simulate the unaccommodated state for distance vision to accommodation for near vision with applied pre-stress fields obtained from an initial process that activates the isolated lens shape into the unaccommodated state. The roles of each individual zonular group as well as the effect of the vitreous membrane and anterior hyaloid membrane on accommodation were investigated.

2. Methods

The three-dimensional model of the whole eye includes the cornea, the sclera, the choroid and the major components involved in accommodation, *i.e.*, the lens, ciliary body and five groups of zonular fibres (Fig. 1a and 1b). The lens model consists of the lens nucleus, lens cortex and lens capsule. The zonular system includes the anterior zonular fibre, the equatorial zonular fibre, the posterior zonular fibre, the vitreous zonule which connects the ciliary body to the anterior hyaloid membrane and the pars plana zonule (Fig. 1c), identified in accordance with the nomenclature of Bassnett [1]. Structures like the iris and the optic disc were not considered as they have no known functional role in accommodation.

2.1. Model geometry

The geometric parameters used to develop the lens model were based on a 35-year-old human eye lens according to our previous study [29]. Geometric parameters of the ciliary body taken from Knaus et al. [23], were originally from an *in vivo* morphological observation of the ciliary muscle using Optical Coherence Tomography (OCT) and Ultrasound Biomicroscopy (UBM) [4,5,30]. The choroidal size and partial parameters of the sclera taken from Knaus et al. [23], were originally from high-field micro-MRI imaging of human eye globes [31]. Geometric parameters of the cornea were taken from Cabeza-Gil et al. [22] Details of all components of the developed eye model are provided in Table 1.

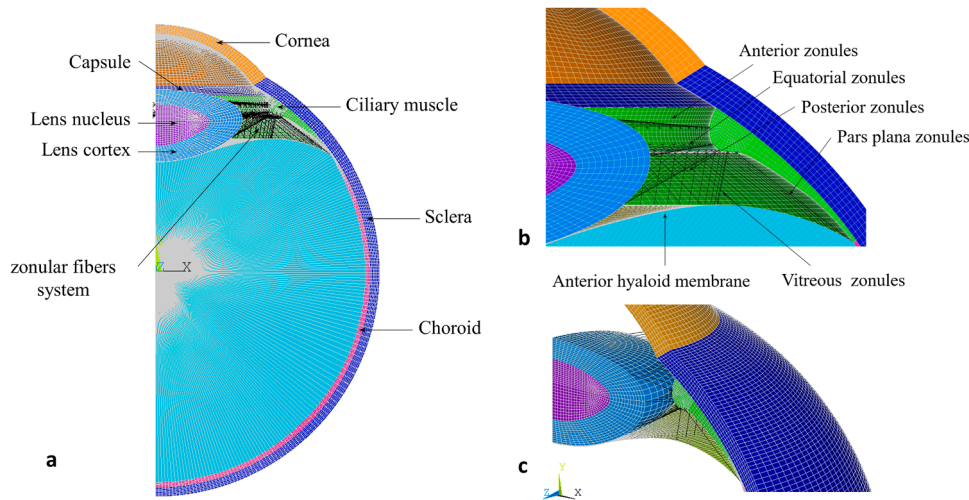


Fig. 1. (a) Model structure diagram in front view and zonular fibres system partial diagram in (b) front view and (c) inclined view.

Table 1

Geometric parameters used to construct the eye model.

tissue	Value(mm)	Source
Lens cortex anterior thickness	0.88	Wang et al. [29]
Lens nucleus anterior thickness	0.90	Wang et al. [29]
Lens nucleus posterior thickness	1.84	Wang et al. [29]
Lens cortex posterior thickness	0.92	Wang et al. [29]
Lens equatorial diameter	8.94	Wang et al. [29]
Lens nucleus equatorial diameter	5.40	Wang et al. [29]
Cornea thickness at anterior	0.50	Das et al. [32]
Cornea Outer radius	7.80	Cabeza-Gil et al. [22]
Cornea Inner Radius	6.50	Cabeza-Gil et al. [22]
Anterior chamber depth	3.10	Mousavi et al. [33]
Sclera thickness at equator	0.50	Das et al. [32]
Sclera Outer radius	12.25	Knaus et al. [23]
Sclera thickness at ora serrata	0.59	Knaus et al. [23]
Ciliary muscle length	4.60	Knaus et al. [23]
Ciliary muscle length: spur to apex	0.88	Knaus et al. [23]
Ciliary muscle thickness at apex	0.72	Knaus et al. [23]
Ciliary muscle thickness at 25% length	0.54	Knaus et al. [23]
Ciliary muscle thickness at 25% length	0.33	Knaus et al. [23]
Ciliary muscle thickness at 25% length	0.16	Knaus et al. [23]
Choroid thickness at equator	0.27	Knaus et al. [23]

2.2. Material properties

The cornea and sclera were considered with a neoHookean hyperelastic material model according to Eq. (1) using material constants from Cabeza-Gil et al. [22] (listed in Table 2).

Table 2

Material properties used to construct the eye model.

tissue	E(MPa)	ν	μ (MPa)	D (Mpa ⁻¹)	Source
Cornea			0.44528	0.19413	Cabeza-Gil et al. [22]
Sclera			0.20546	0.08971	Cabeza-Gil et al. [22]
Choroid	0.6	0.49			Wang et al. [38]
Ciliary muscle	0.006	0.49			Liu et al. [39]
Lens cortex	0.002607	0.49			Wilde et al. [34]
Lens nucleus	0.000776	0.49			Wilde et al. [34]
Lens capsule	4.9	0.47			Wang et al. [29]
zonular fibres	0.35	0.47			Wang et al. [29]

$$W = \frac{\mu}{2}(\bar{I}_1 - 3) + \frac{1}{D}(J - 1)^2 \quad (1)$$

Each component of the lens was modelled with linear elastic, isotropic, and homogeneous materials. The elastic moduli assigned to the nucleus and cortex of lens were taken from measurements of Wilde et al. [34], who used the non-destructive spinning lens method to determine the elasticities of the nucleus and cortex. The lens was considered as nearly incompressible [35–37] with a Poisson's ratio of 0.49 for the lens and 0.47 for the lens capsule and zonular fibres [29]. (Poisson's ratio is a measure of the compression in one direction when a material is being stretched in the perpendicular direction and has an upper limit of 0.5 when the material is incompressible. A Poisson's ratio of 0.49 applies to almost incompressible behaviour and has been widely used in modelling studies of eye lenses [16–18,28,29].) Detailed material properties of each part are shown in Table 2. The ciliary body and the choroid were also assumed to be of linear elastic and isotropic homogeneous materials. Young's modulus of the choroid was taken from a previous study [38] whilst Young's modulus of the ciliary body was determined according to the elasticity ratio between the lens and the ciliary body as used in the eyeball model for rupturing analysis by Liu et al. [39].

2.3. FE model development

The FE model was developed in ANSYS Mechanical APDL (ver. 2021a). Considering the symmetry, a quarter model of the eye was established to reduce calculation time by treating the optical axis as the axis of symmetry.

The major components of the model, including the cornea and the sclera, the choroid, the lens nucleus, the lens cortex and the ciliary muscle were meshed using 8-node brick elements (ANSYS element type: SOLID 185) using the reduced integration method. The lens capsule and the anterior hyaloid membrane were meshed using 4-node shell elements (ANSYS element type: SHELL 181) with membrane stiffness only. The different groups of zonular fibres were meshed using 2-node link elements (ANSYS element type: LINK 180) with tensional behaviour only. Each zonular fibre was meshed with a single LINK180 element and was assigned with a cross-sectional area of 0.012mm², the length of the anterior, equatorial, posterior, vitreous and pars plana zonules are 2.225 mm, 1.520 mm, 2.613 mm, 1.288 mm, 3.540 mm, respectively. The vitreous has a physiological role in maintaining intraocular pressure and was modelled using 5-node three-dimensional hydrostatic elements (ANSYS element type: HSFLD 242) with incompressible fluid behaviour. The total number of elements and total number of nodes of the

developed quarter model is 119,050 and 121,829, respectively. Symmetric boundary conditions were added to the planes of symmetry, and the three translational degrees of freedom were constrained for nodes located on the outer scleral surface of the model. Nonlinear geometrical analysis was performed for all simulations to consider the large deformation effect.

2.4. Establishment of pre-stress approach and initial simulations

The present study has proposed a lens pre-stress modelling approach to simulate the unaccommodated state for distance vision to accommodation for near vision, mimicking the process by which the lens returns from a relatively flattened shape to a more spherical shape. The lens geometry used in the present study was taken from optical measurements of the isolated lens [40] that had been freed from any zonular tension. A fully accommodated lens *in vivo*, however, may still be under minimal tension to keep the lens in a physiologically stable position. To address this concern, an initial simulation for obtaining the pre-stress field of the lens model was performed by simulating deformations of the lens from its fully stress-free state to a stressed, unaccommodated state (Fig. 2a). To do this, the lens model, which includes the lens nucleus, the lens cortex and the anterior, equatorial and posterior zonular fibres, was firstly isolated from the whole eye model and displacements were applied to the endpoints of the three zonular fibre groups to mimic around 6.5 dioptres of optical change, which is the accommodative capacity that can be expected of a lens in the 4th decade of life (Fig. 2b). The anterior zonule was angled posteriorly at 16°, the equatorial zonule was along the horizontal direction and the posterior zonule was given an anterior incline of 21°. Displacements of 0.42 mm, 0.315 mm, and 0.35 mm were applied to the anterior, equatorial, posterior zonules respectively, along their fibre orientations. The anterior, equatorial, posterior zonules had lengths of 2.198 mm, 1.104 mm and 2.239 mm, respectively. The element type and material parameters were as same as the whole eye models described above.

Nonlinear geometrical analysis was performed to consider the large deformation effect. The six stress components (three normal stresses and three shear stresses) and the deformed coordinates of each node taken from the flattened lens model resulted from above simulations were treated as inputs/pre-stresses to the full anterior eye model used for the formal simulation.

2.5. Mesh convergence analysis

A mesh convergence analysis was conducted to ensure that the mesh density met the calculation requirements. A total of 4 models with different mesh densities (971, 2583, 18,623 and 113,423 elements) were created (Figs. 3a-d). The test results showed that the displacements at the equator, the anterior and posterior pole tended to converge with the

model of 18,623 elements (Figs. 3e-g). This mesh density was used for formal analysis in the present study.

2.6. Simulations and data analysis

The pre-stressed lens component obtained from the initial simulations was then assembled with the anterior eye model so that during the formal simulation, the lens would release its internal stresses and transmit tensions to its surrounding tissues including the five groups of zonular fibres and the ciliary muscle until an equilibrium state is reached. During this process, the lens returned from an unaccommodated state to an accommodated state (Fig. 4a).

To investigate the contributions of each group of zonular fibres, one out of the five zonular groups was eliminated in sequence, creating additional five models with different zonular components (Figs. 4b-f): a model without the anterior zonular fibres (AZ cut), a model without the equatorial zonular fibres (EZ cut), a model without the posterior zonular fibres (PZ cut), a model without the vitreous zonules (VZ cut), and a model without the pars plana zonules (PPZ cut). The lens deformation and changes in zonular tension of the five models with different zonular configurations were compared with the results of the model with all five groups of zonular fibres (ALL). Parameters describing the lens deformation, *i.e.*, the radii of curvature of the anterior and posterior surfaces (Ra and Rp) as well as the sagittal plane thickness (T) of both the whole lens and the lens nucleus, were calculated using the nodal coordinates of the nodes extracted from the corresponding surfaces of the lens model within the central 6 mm zone [41]. The above parameters were used to build the lens optical model in ZEMAX OpticStudio (ver. 20.3.2) to calculate the effective focal length of the lens. The lens optical model consists of four major surfaces, the anterior lens surface, the anterior nuclear surface, the posterior nuclear surface and the posterior lens surface. The nuclear and the cortical region were assigned refractive index values of 1.406 and 1.391 respectively, according to a previously reported 35-year-old optical model [42]. The Central Optical Power (COP) of the lens was determined by calculating the reciprocal of the effective focal length of the lens optical model. For each model, the change of anterior and posterior radii of curvature in response to changes in COP was fitted by linear regression analysis. The standard *t*-test analysis (using a significance level of 0.05) for comparing two independent slopes was performed between modelled results and *in vivo* published data from OCT measurement of 13 young subjects who responded to accommodative stimuli up from 0 to 6D, in 1.5D steps [41].

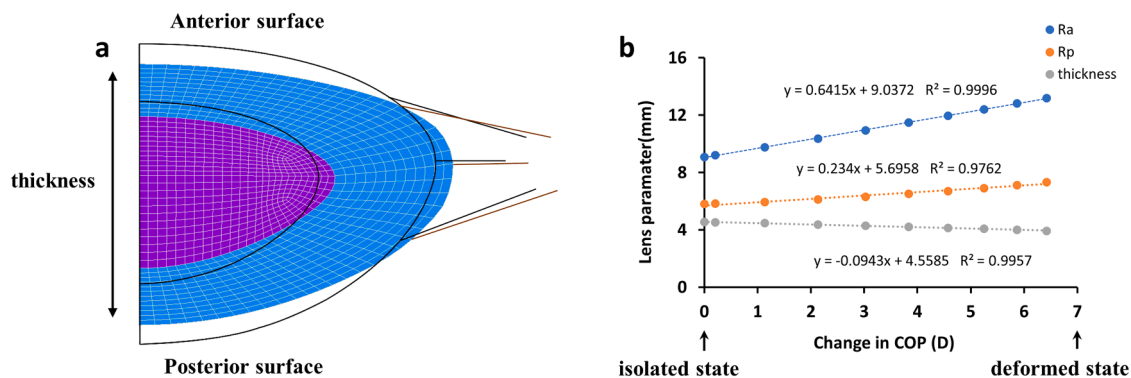


Fig. 2. (a) Deformation of the lens model under stretching of three sets of zonules during initial simulation (black line indicates undeformed shape) and (b) resultant changes in thickness as well as anterior and posterior radius of curvature up to 6 dioptres change in optical power.

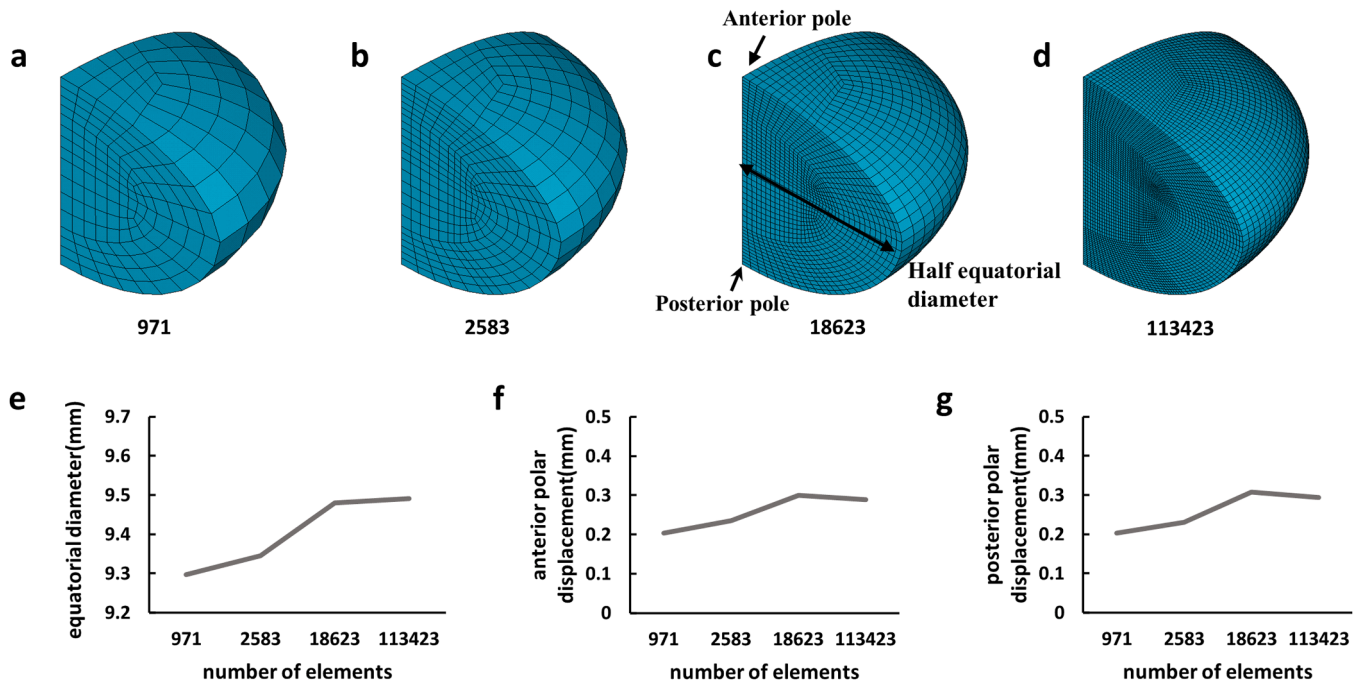


Fig. 3. The lens models with different mesh densities (a) model with 971 elements, (b) model with 2583 elements, (c) model with 18,623 elements, (d) model with 113,423 elements, and the simulated change in (e) equatorial diameter, (f) anterior polar displacement and (g) posterior polar displacement with increasing mesh densities.

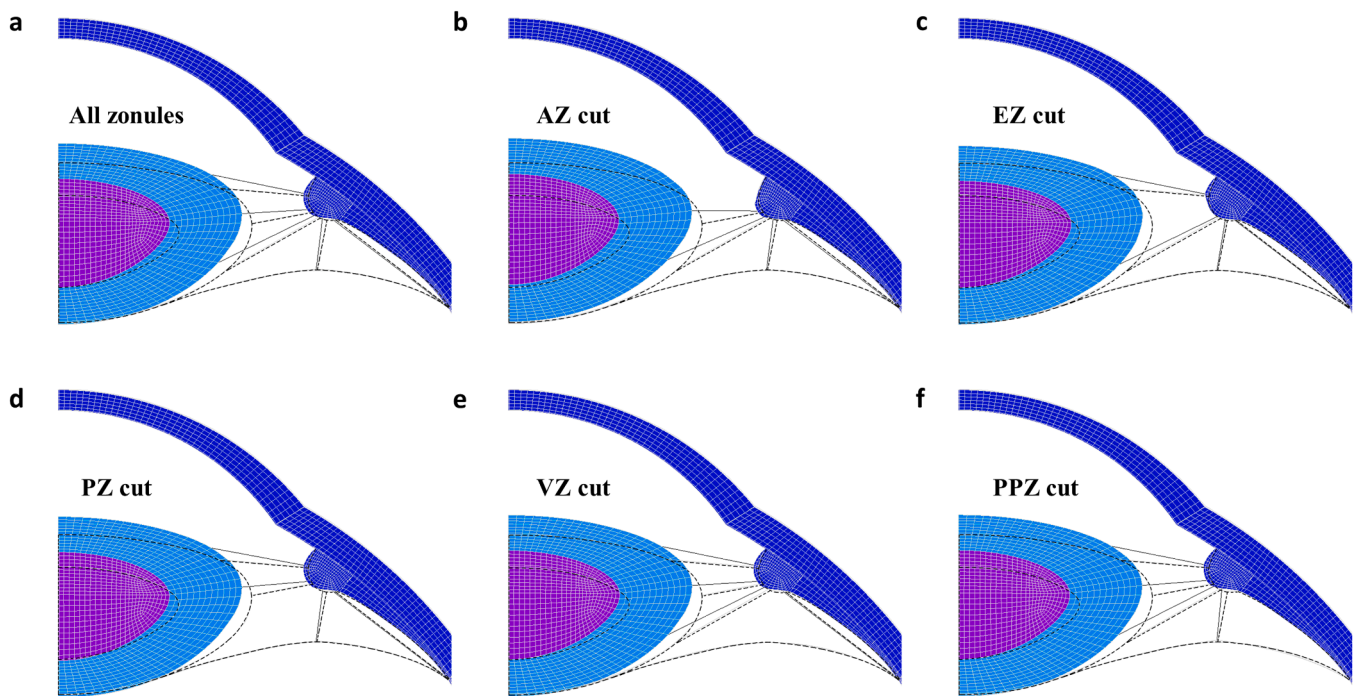


Fig. 4. The deformed and undeformed models with different zonular arrangements (the black dashed line represents the undeformed edge). (a) the model with all five groups of zonules; (b) the model without the anterior zonules; (c) the model without the equatorial zonules; (d) the model without the posterior zonules; (e) the model without the vitreous zonules; (f) the model without the pars plana zonules. (AZ: anterior zonule, EZ: equatorial zonule, PZ: posterior zonule, VZ: vitreous zonule, PPZ: pars plana zonule).

3. Results

3.1. Changes in lens shape

During simulated accommodation, the components of the model

underwent different levels of deformation and the lens returned from a relatively flattened shape to a more spherical shape with little displacement seen at the posterior pole (Fig. 4a). Notably, there is an inconsistency in lens shape between the isolated state and the accommodated state as seen the parameters listed in Table 3. Changes in

Table 3

The parameters of lens in the isolated state and in the accommodated state with different zonular fibres groups.

	Ra/mm	Rp/mm	Equatorial diameter/mm	Thickness/mm
Isolated	9.081	5.799	8.940	4.540
ALL	10.060	5.835	9.044	4.457
A	9.263	5.839	9.026	4.517
E	10.931	6.047	9.058	4.393
P	10.042	5.922	9.042	4.452
V	10.059	5.832	9.044	4.459
PP	10.032	5.847	9.030	4.462

anterior radius of curvature (Ra), posterior radius of curvature (Rp) and sagittal thickness of the model with all five groups of zonular fibres, plotted against changes in COP, were compared with those reported in an *in vivo* study [41] (Fig. 5). There is no statistically significant difference between modelled results and the *in vivo* measurements for the anterior radius of curvature ($p = 0.6567$). However, statistical differences were found for the posterior radius of curvature ($p = 0.0179$) and the sagittal thickness ($p = 0.0058$).

Changes in the shape parameters of the deformed lens models plotted against the changes in the COP for the model with all five zonular fibres as well as for the five models with one zonular part eliminated are shown in Fig. 6. The shape parameters of the models follow the same trend with increasing change in COP: both the anterior and posterior radii of curvature decrease as the change in COP increases, with higher rate of change seen for the anterior radius of curvature than for the posterior radius of curvature (Figs. 6a,b). With accommodation, the anterior pole moves forward (Fig. 6e), the posterior pole moves backward (Fig. 6f), and the anterior polar displacement is greater than that of the posterior pole. The lens sagittal thickness increases while the equatorial diameter decreases with accommodative change (Figs. 6c,d). Lenses in all six models show similar trends in simulated shape change.

To compare the functional differences between the zonules, parameters related to lens shape in all six models were compared (Fig. 7). The optical power change is the highest with simulated shape change in the anterior zonular-cut model and is the lowest in the equatorial zonular-cut model. The amount of change in COP is almost identical between the model with all zonules and the rest three models (Fig. 7a). Change in COP in the all-zonules model (5.313D) is lower than that in the anterior zonular-cut model (5.966D) but is higher than that in the equatorial zonular-cut model (4.305D). The anterior radius of curvature shows the lowest value in the anterior zonular-cut model but the highest value in the equatorial zonular-cut model (Fig. 7b). The posterior radius of curvature of the equatorial and posterior zonular-cut models are higher than those of the other models (Fig. 7c). The thickness variations amongst different models (Fig. 7d) are similar to the changes in COP shown in Fig. 7a. The equatorial diameter is lowest in the anterior zonular-cut model and highest in the equatorial zonular-cut model

(Fig. 7e). The anterior zonular-cut model shows the highest anterior polar displacement whilst this value is lowest in the equatorial zonular-cut model (Fig. 7f). Changes in the anterior and posterior radii of curvature and thickness per dioptre can be quantified using the slope of linear regression lines (Figs. 7g, h, i). Compared with the all-zonules model, the anterior zonular-cut model shows a higher anterior slope but lower posterior slope, the equatorial zonular-cut model shows a lower anterior slope, higher posterior slope and much higher thickness slope (Fig. 7g, h, i). Overall, vitreous and pars plana zonular-cut models show similar results to those of the all-zonules model.

3.2. Changes in zonular tension

To investigate how the zonular system transmits tension from the ciliary body to the lens, the average axial strain and the average axial stress of each zonular set in all six models in the fully accommodated state were obtained (Figs. 8). The stress and strain values of all zonules were averaged because numerical calculations cannot give exactly the same values amongst different zonules (The standard deviations of stresses and of strains vary between 0.00003Mpa to 0.00105Mpa and between 0.00011 to 0.00300 amongst different zonular cut models).

The circumferential sum of axial force (on a 360-degree full model basis) in all models were listed in Table 4. In the all-zonules model, the anterior and equatorial zonular fibres carry most of the tension and strain, the posterior and pars plana zonular fibres carry relatively lower amounts of tension and strain; the vitreous zonules seem to have negligible impact (Figs. 8a). In the anterior zonular-cut model, tension and strain in the equatorial zonules increases (Figs. 8b) whilst in other zonular-cut models, the distributions of tension and strain amongst different zonular groups show little variation (Figs. 8c,d,e,f).

At the end of simulation when the model entered the maximum accommodated state, the equatorial zonular tension in the anterior zonular-cut model is higher than that in the all-zonules model. Conversely, the posterior zonular tension in the anterior zonular-cut model is lower than that in the all-zonules model. The anterior zonular tension in the equatorial zonular-cut model is slightly higher than that in the all-zonules model. The posterior zonular tension in the equatorial zonular-cut model is higher than in the all-zonules model (Table 4).

3.3. Deformation of the ciliary body

The Anterior Ciliary body Length (ACL) and the maximum width of the ciliary body (CMmax) before and after the simulation were determined (Fig. 9a). Changes in both the ACL and the CMmax during accommodation, as simulated in the present study, were compared with the *in vivo* measured data reported by Sheppard and Davies (2010) [30]. Changes in ACL simulated by the models are similar to those measured *in vivo* on the temporal side [30]. It should be noted the CMmax in the

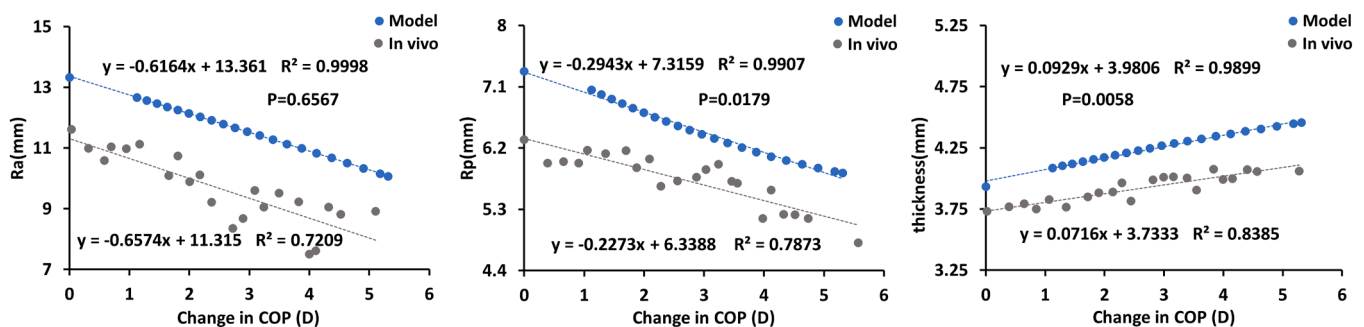


Fig. 5. The change in (a) anterior radii of curvature, (b) posterior radii of curvature and (c) sagittal plane thickness for the model ALL and *in vivo* study with change in COP. Statistical *t*-test for comparing two independent slopes was performed between modelled results and *in vivo* measured data for each displayed parameters with *p* values displayed in each figure.

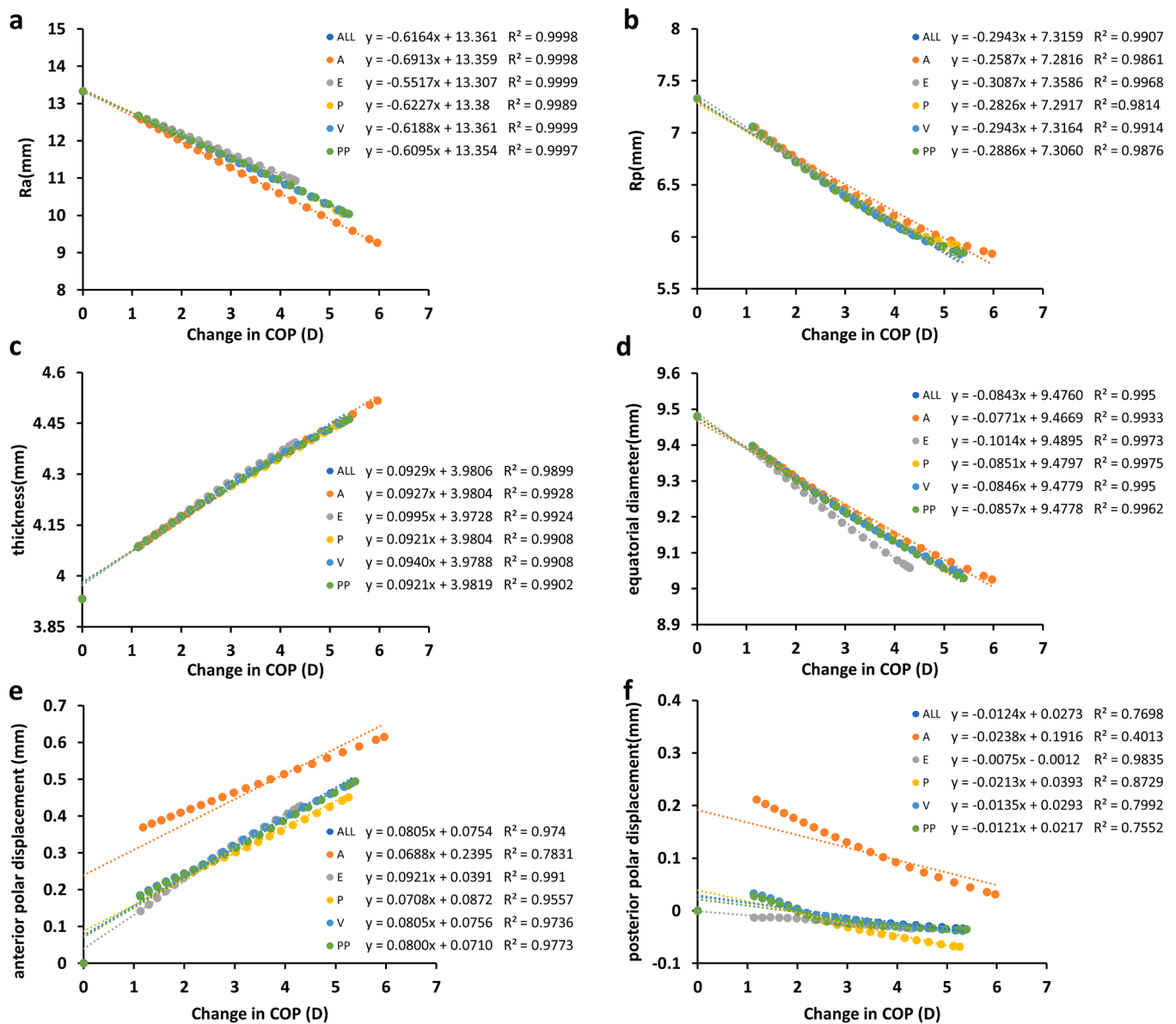


Fig. 6. The change in (a) anterior radii of curvature, (b) posterior radii of curvature, (c) sagittal thickness, (d) equatorial diameter, (e) anterior polar displacements, and (f) posterior polar displacements plotted against change in COP. (ALL: The model with all five groups of zonules, A: the model without the anterior zonules, E: the model without the equatorial zonules, P: the model without the posterior zonules, V: the model without the vitreous zonules, PP: the model without the pars plana zonules).

present study was compared with the *in vivo* measured CM25 [30] which represents the ciliary muscle width at 25% of the overall ciliary muscle length (Table 5). Comparisons in von Mises stress distribution in the ciliary body were made between the all-zonules model (Fig. 9b) and the five zonular-cut models (Figs. 9c to 9g). In the anterior zonular-cut model (Fig. 9c), stresses in the anterior end of the ciliary body are of lower magnitude than those in the all-zonules model (Fig. 9b), while in the equatorial and pars plana zonular-cut models (Figs. 9d,g), stresses in the pars plana region do not show the high magnitudes that are seen in the all-zonules models.

4. Discussion

In the present study, the contributions of five groups of zonular fibres (including the anterior, the equatorial, the posterior, the vitreous and the pars plana zonules) to accommodation have been investigated by adopting the classical control variables method. A pre-stressed

modelling approach was proposed to simulate the positive accommodative process that alters the visual focus from far to near. In total, six models were developed by removing one of the five zonular groups in each model and treating the model with all five zonular groups as the reference model. Results of the five zonular-cut models were compared with that of the all-zonules model. The reference model demonstrated a series of accommodative changes that are comparable with those reported previously [41,43,44], mainly occur in the lens section, *i.e.*, the anterior and posterior surface curvature as well as the sagittal thickness increased with a concomitant forward movement of the anterior pole, whilst the equatorial diameter decreased. These changes in lens shape contribute to an increase in the COP. The cornea demonstrated negligible change in thickness and curvature with simulated accommodation.

Previously *in vivo* observations of ciliary body movement, such as using pharmacologically induced accommodation imaged by ultrasound microscopy [4,5] and by anterior segment OCT [30], reported consistent findings: the apex of the ciliary body moves anteriorly and inward

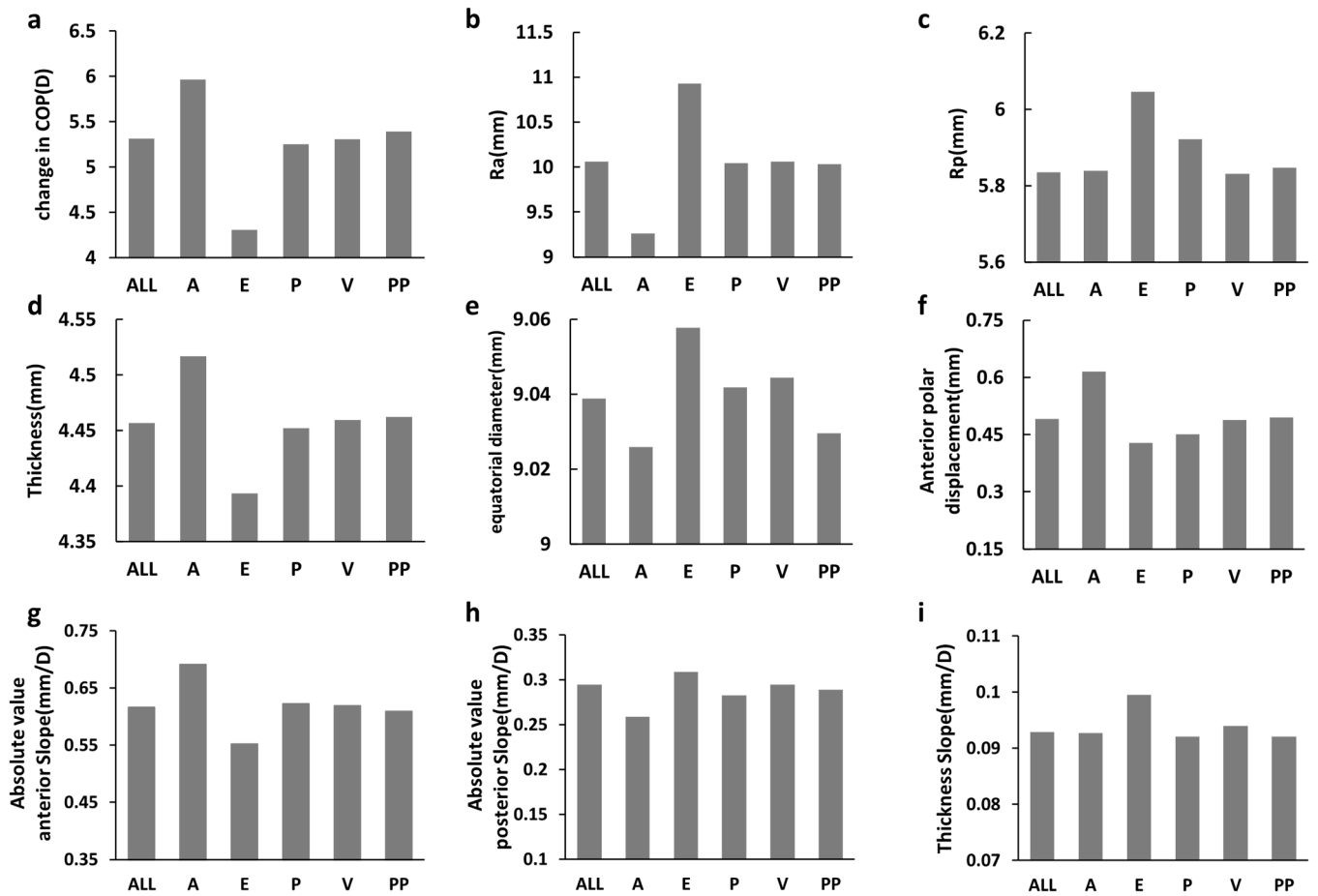


Fig. 7. The parameters related to lens shape in six models, (a) change of COP, (b) the anterior radius of curvature, (c) the posterior radius of curvature, (d) the thickness, (e) the equatorial diameter, (f) the anterior pole displacement, (g) absolute value of the anterior slope, (h) absolute value of the posterior slope, (i) the thickness slope. (ALL: The model with all five groups of zonules, A: the model without the anterior zonules, E: the model without the equatorial zonules, P: the model without the posterior zonules, V: the model without the vitreous zonules, PP: the model without the pars plana zonules).

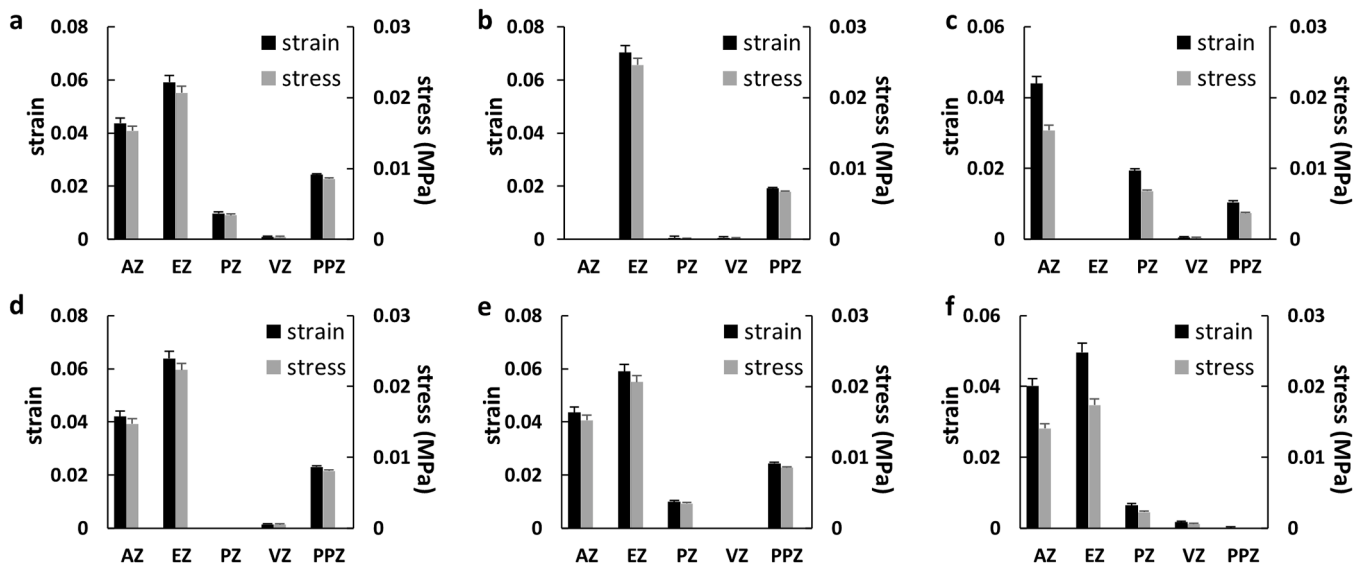


Fig. 8. The average axial strain and the average axial stress of each zonular set in all six models, (a) all-zonules model, (b) anterior zonular-cut model, (c) equatorial zonular-cut model, (d) posterior zonular-cut model, (e) vitreous zonular-cut model, and (f) pars plana zonular-cut models. (AZ: anterior zonule, EZ: equatorial zonule, PZ: posterior zonule, VZ: vitreous zonule, PPZ: pars plana zonule).

Table 4
The circumferential sum of axial force of each zonular set in all six models.

Circumferential axial force (mN)	AZ	EZ	PZ	VSZ	VLZ
ALL	14.160	18.844	3.272	0.330	8.007
A		22.159	0.010	0.104	6.336
E	14.233		6.392	0.156	3.479
P	13.645	20.255		0.522	7.579
VS	14.100	18.797	3.352		8.016
VL	13.077	15.992	2.199	0.584	

during distance vision to accommodation for near vision. Such deformation was also produced by the whole eye model developed in the present study. The values of elastic modulus reported in the literature cover a wide range and this could be attributed to the variety of tissue handling means and different measurement techniques [19]. The present study has used a linear elastic material model taking Young’s moduli measured by spinning the lens [34]. The results of the model are consistent with experimental measurements [4,5,30,41,43].

Results presented in this study show that the anterior zonular fibre has a negative effect on lens accommodative changes because the model without this zonular group has higher changes in optical power than that of the reference model. The equatorial zonular fibre has a positive effect on accommodation because the model without the equatorial zonules demonstrates lower changes in optical power. The model without the posterior zonular fibre produces a lower change in COP while the model without the pars plana zonules produces a higher change in COP, both slightly, than does the reference model, which indicates the positive effect of posterior zonular set and the negative effect of pars plana zonules on accommodation. It can be clearly seen that the contribution to change in optical power by the equatorial zonular fibre is much larger than by the posterior zonular fibre (Fig. 7). The vitreous zonules and the pars plana zonules seem to have little effect on the lens optical power change. The anterior and the equatorial zonular fibres have the major influence on lens power change. However, the pars plana zonular fibres appear to have an important effect on the deformation of the ciliary body, for when these zonular fibres are absent, the stress at the posterior end of the pars plana decreases significantly (Fig. 9). The pars plana zonules pull the pars plana during accommodation and limit the forward movement of the ciliary process. This is also found in *in vivo* studies in primates: lysis of the pars plana zonular fibre leads to the increase in

forward movement of the ciliary muscle apex and in muscle width [45]. An additional finding was observed during *in vivo* OCT examination of the human eye: during accommodation the choroid around the optic nerve thinned and moved centrifugally [46], suggesting that the influence of vitreous system cannot be ignored during ciliary muscle movement.

This work reveals functional differences between different groups of zonular fibres using computational models assuming that the ocular structures are symmetric about the central optical axis. Spatial variations in zonular tension related to the tilting of the human lens [47,48] as well as to spatial changes in the ciliary muscle [30] have been noted. These are worthy of investigation in future modelling studies that consider individual parametric variations.

The sum of the zonular forces at the end of simulation ie maximum accommodation was 44.61mN which concurs with the value of 55.81mN reported in a previous *in vitro* stretching experiment on a 47-year-old human eye [25]. In other simulation studies, the mean value of the total net force delivered by the zonular fibres and ciliary muscle in a 29-year-old lens model with different material properties was 56mN [49], the zonular force in this paper is similar to the results obtained from previous studies.

In an *in vitro* stretching study of cynomolgus monkey lens, Nankivil et al. [50] found that in the absence of the anterior and equatorial zonules, 69% of the change in optical power is retained, which suggested that the posterior zonules and anterior hyaloid membrane play a significant role in accommodation. However, this study did not evaluate the individual role of different zonules and the *in vitro* stretching

Table 5
The accommodative changes of ciliary muscle dimensions.

		Ciliary muscle dimensions	
		ACL	CMmax
Sheppard	Nasal	-9.30%	2.80%
	Temporal	-17.78%	3.82%
ALL		-17.88%	2.03%
A		-21.22%	4.84%
E		-29.07%	-0.53%
P		-18.12%	1.97%
V		-17.87%	2.06%
PP		-17.37%	2.47%

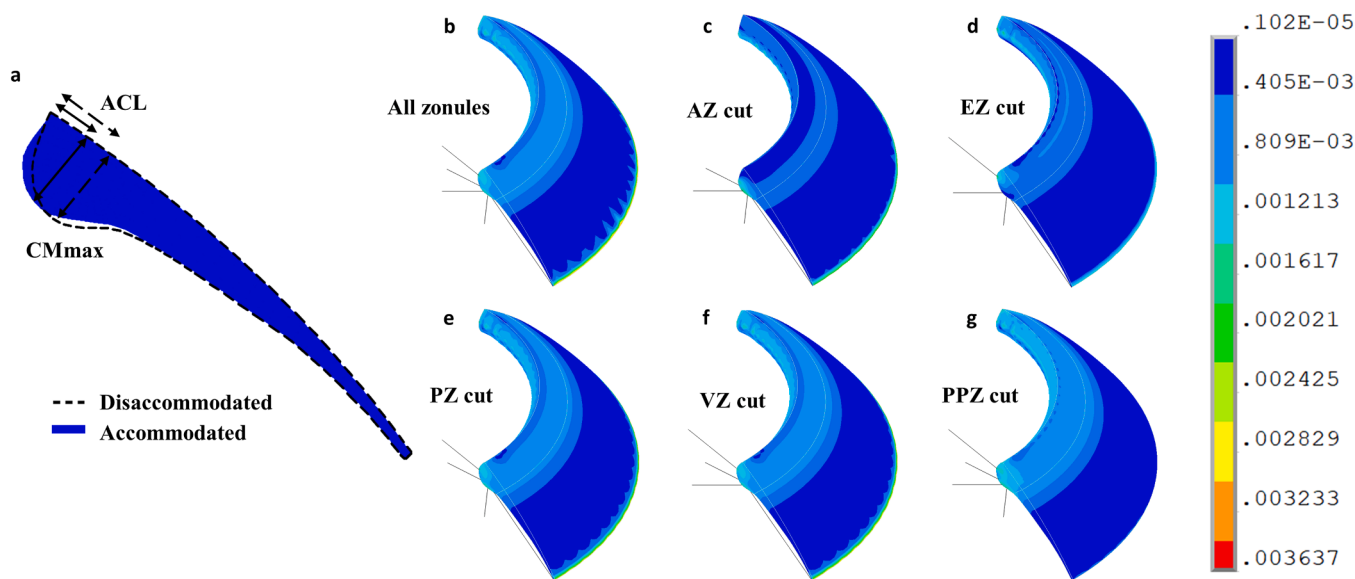


Fig. 9. The shape of ciliary muscle, (a) the dotted line represents the outline in unaccommodated state, and blue solid represents the shape in accommodated state, the dotted and solid arrows stand for CM parameters in unaccommodated state and accommodated states respectively. The stress distribution (von Mises stress in MPa) of the ciliary muscle (b-g), from left to right are the results of the all- zonular model and the vitreous and pars plana zonular-cut models, respectively.

experiment involved destructive operations to the eyeballs that would have altered the lens deformation [50]. The simulations in the present study, confirm that the anterior zonules have a greater effect on the anterior lens surface while the posterior zonules have a greater effect on the posterior lens surface; in accordance with the findings of an *in vitro* stretching experiment [51]. In addition, simulation results show that the rate of change in radius of curvature per dioptre and the polar displacement are higher on the anterior surface than on the posterior surface, which concurs with previous *in vivo* observations [43,52]. Displacement of the posterior pole during accommodation is almost negligible, suggesting that the anterior curvature predominantly contributes to the change in power during accommodation of the lens. Although statistical differences were found for the posterior radius of curvature and the sagittal thickness, the model provides a closer relationship between the anterior surface and the *in vivo* measurements [41].

When the anterior zonular fibres were removed, in the fully accommodated state there was an increase in the equatorial zonular tension and a decrease in posterior zonular tension (Table 4) and a resultant increase in COP (Fig. 7). When the equatorial zonular fibre was removed, the anterior zonular tension in the fully accommodated state increased slightly while the posterior zonular tension increased significantly (Table 4) and this resulted in a decrease in the change of COP (Fig. 7). The results, which show that the increase in equatorial zonular tension alone would increase accommodation, suggest that the equatorial zonular fibres are active contributors to increasing the lens optical power during accommodation. The importance of the anterior zonular fibres in the accommodative process has been demonstrated in a number of previous studies [53]. For instance, the apparent anterior shift of this part of the zonule with age [54,55] has been considered as a contributing factor to the onset of presbyopia [54]; the abnormality of the anterior zonules has been associated with ocular abnormalities or disease including higher intraocular pressure and plateau iris configuration [56,57]; the angle of anterior and posterior zonules affects the accommodative response [18]. Findings from these studies suggest that the functions of the anterior zonules may be more complex and vital for accommodation than has been considered thus far. Future work is needed to investigate a wider range of factors with more sophisticated and physiologically relevant models.

Declaration of Competing Interest

None Declared.

Funding

This work was supported by National Natural Science Foundation of China (Grants No: 12372301, 82000878), the Fundamental Research Funds for the Central Universities and the Opto-Biomechanical Eye Research Network OBERON Marie Skłodowska-Curie Action (MSCA) Innovative Training Network (ITN) EU MSCA-ITN-ETN proposal number 956720.

References

- [1] S. Bassnett, Zinn's zonule, *Prog. Retin. Eye Res.* 82 (2021), 100902, <https://doi.org/10.1016/j.preteyeres.2020.100902>.
- [2] G. Raviola, The fine structure of the ciliary zonule and ciliary epithelium. With special regard to the organization and insertion of the zonular fibrils, *Invest. Ophthalmol. Vis. Sci.* 10 (11) (1971) 851–869.
- [3] J.W. Rohen, Scanning electron microscopic studies of the zonular apparatus in human and monkey eyes, *Invest. Ophthalmol. Vis. Sci.* 18 (2) (1979) 133–144.
- [4] M.A. Croft, M.T. Nork, J.P. McDonald, A. Katz, E. Lütjen-Drecoll, P.L. Kaufman, Accommodative movements of the vitreous membrane, choroid, and sclera in young and presbyopic human and nonhuman primate eyes, *Invest. Ophthalmol. Vis. Sci.* 54 (7) (2013) 5049–5058, <https://doi.org/10.1167/iov.12-10847>.
- [5] M.A. Croft, J.P. McDonald, A. Katz, T.L. Lin, E. Lütjen-Drecoll, P.L. Kaufman, Extralenticular and lenticular aspects of accommodation and presbyopia in human versus monkey eyes, *Invest. Ophthalmol. Vis. Sci.* 54 (7) (2013) 5035–5048, <https://doi.org/10.1167/iov.12-10846>.
- [6] M.A. Croft, G. Heatley, J.P. McDonald, A. Katz, P.L. Kaufman, Accommodative movements of the lens/capsule and the strand that extends between the posterior vitreous zonule insertion zone & the lens equator, in relation to the vitreous face and aging, *Ophthalmic Physiol. Opt.* 36 (1) (2016) 21–32, <https://doi.org/10.1111/opo.12256>.
- [7] H. Helmholtz, Ueber die accommodation des Auges, *Archiv für Ophthalmologie* 1 (1855) 1–74, <https://doi.org/10.1007/BF02720789>.
- [8] W. Peddie, Helmholtz's treatise on physiological optics, *Nature* 118 (1926) 74–76, <https://doi.org/10.1038/118074a0>.
- [9] R.A. Schachar, Cause and treatment of presbyopia with a method for increasing the amplitude of accommodation, *Ann. Ophthalmol.* 24 (12) (1992) 445–452.
- [10] R.A. Schachar, Zonular function: a new hypothesis with clinical implications, *Ann. Ophthalmol.* 26 (2) (1994) 36–38.
- [11] D.J. Coleman, Unified model for accommodative mechanism, *Am. J. Ophthalmol.* 69 (6) (1970) 1063–1079, [https://doi.org/10.1016/0002-9394\(70\)91057-3](https://doi.org/10.1016/0002-9394(70)91057-3).
- [12] D.P. Piñero, Technologies for anatomical and geometric characterization of the corneal structure and anterior segment: a review, *Semin. Ophthalmol.* 30 (3) (2015) 161–170, <https://doi.org/10.3109/08820538.2013.835844>.
- [13] A. Konstantopoulos, P. Hossain, D.F. Anderson, Recent advances in ophthalmic anterior segment imaging: a new era for ophthalmic diagnosis? *Br. J. Ophthalmol.* 91 (4) (2007) 551–557, <https://doi.org/10.1136/bjo.2006.103408>.
- [14] H.J. Burd, S.J. Judge, M.J. Flavell, Mechanics of accommodation of the human eye, *Vision Res.* 39 (9) (1999) 1591–1595, [https://doi.org/10.1016/S0042-6989\(98\)00298-3](https://doi.org/10.1016/S0042-6989(98)00298-3).
- [15] R.A. Schachar, A.J. Bax, Mechanism of human accommodation as analyzed by nonlinear finite element analysis, *Compr. Ther.* 27 (2) (2001) 122–132, <https://doi.org/10.1007/s12019-996-0006-5>.
- [16] E.A. Hermans, M. Dubbelman, G.L. van der Heijde, R.M. Heethaar, Estimating the external force acting on the human eye lens during accommodation by finite element modelling, *Vision Res.* 46 (21) (2006) 3642–3650, <https://doi.org/10.1016/j.visres.2006.04.012>.
- [17] K. Wang, D. Venetsanos, J. Wang, B.K. Pierscionek, Gradient moduli lens models: how material properties and application of forces can affect deformation and distributions of stress, *Sci. Rep.* 6 (2016) 31171, <https://doi.org/10.1038/srep31171>.
- [18] K. Wang, D.T. Venetsanos, J. Wang, A.T. Augousti, B.K. Pierscionek, The importance of parameter choice in modelling dynamics of the eye lens article, *Sci. Rep.* 7 (1) (2017) 16688, <https://doi.org/10.1038/s41598-017-16854-9>.
- [19] K. Wang, B.K. Pierscionek, Biomechanics of the human lens and accommodative system: functional relevance to physiological states, *Prog. Retin. Eye Res.* 71 (2019) 114–131, <https://doi.org/10.1016/j.preteyeres.2018.11.004>.
- [20] K. Wang, D.T. Venetsanos, M. Hoshino, K. Uesugi, N. Yagi, B.K. Pierscionek, A modeling approach for investigating opto-mechanical relationships in the human eye lens, *IEEE Trans. Biomed. Eng.* 67 (4) (2020) 999–1006, <https://doi.org/10.1109/TBME.2019.2927390>.
- [21] R.P. Wilkes, M.A. Reilly, A pre-tensioned finite element model of ocular accommodation and presbyopia, *Int. J. Adv. Eng. Sci. Appl. Math.* 8 (1) (2016) 25–38, <https://doi.org/10.1007/s12572-015-0141-2>.
- [22] I. Cabeza-Gil, J. Grasa, B. Calvo, A validated finite element model to reproduce Helmholtz's theory of accommodation: a powerful tool to investigate presbyopia, *Ophthalmic Physiol. Opt.* 41 (6) (2021) 1241–1253, <https://doi.org/10.1111/opo.12876>.
- [23] K.R. Knaus, A.M. Hipsley, S.S. Blemker, The action of ciliary muscle contraction on accommodation of the lens explored with a 3D model, *Biomech. Model. Mechanobiol.* 20 (3) (2021) 879–894, <https://doi.org/10.1007/s10237-021-01417-9>.
- [24] R.F. Fisher, The ciliary body in accommodation, *Trans. Ophthalmol. Soc. U. K.* 105 (1986) 208–219. Pt 2.
- [25] R. Michael, M. Mikielewicz, C. Gordillo, G.A. Montenegro, L. Pinilla Cortés, R. I. Barraquer, Elastic properties of human lens zonules as a function of age in presbyopes, *Invest. Ophthalmol. Vis. Sci.* 53 (10) (2012) 6109–6114, <https://doi.org/10.1167/iov.11-8702>.
- [26] Z.I. Bocskaï, G.L. Sándor, Z. Kiss, I. Bojtár, Z.Z. Nagy, Evaluation of the mechanical behaviour and estimation of the elastic properties of porcine zonular fibres, *J. Biomech.* 47 (13) (2014) 3264–3271, <https://doi.org/10.1016/j.jbiomech.2014.08.013>.
- [27] J.N. Webb, C. Dong, A. Bernal, G. Scarcelli, Simulating the mechanics of lens accommodation via a manual lens stretcher, *J. Vis. Exp.* (132) (2018) 57162, <https://doi.org/10.3791/57162>.
- [28] D. Ljubimova, A. Eriksson, S.M. Bauer, Numerical study of the effect of vitreous support on eye accommodation, *Acta Bioeng. Biomech.* 7 (2005) 3–15, <https://www.researchgate.net/publication/237735941>.
- [29] K. Wang, M. Hoshino, K. Uesugi, N. Yagi, B.K. Pierscionek, Contributions of shape and stiffness to accommodative loss in the ageing human lens: a finite element model assessment, *J. Opt. Soc. Am. A Opt. Image Sci. Vis.* 36 (4) (2019) B116–B122, <https://doi.org/10.1364/josaa.36.00b116>.
- [30] A.L. Sheppard, L.N. Davies, *In vivo* analysis of ciliary muscle morphologic changes with accommodation and axial ametropia, *Invest. Ophthalmol. Vis. Sci.* 51 (12) (2010) 6882–6889, <https://doi.org/10.1167/iov.10-5787>.
- [31] R.E. Norman, J.G. Flanagan, S.M.K. Rausch, I.A. Sigal, I. Tertinegg, A. Eilaghi, S. Portnoy, J.G. Sled, C.R. Ethier, Dimensions of the human sclera: thickness measurement and regional changes with axial length, *Exp. Eye Res.* 90 (2) (2010) 277–284, <https://doi.org/10.1016/j.exer.2009.11.001>.

- [32] S. Das, M. Subashini, FEM modelling of human eye for investigating the thermal effects of tumor on the ocular surface temperature, *ARPN J. Eng. Appl. Sci.* 12 (23) (2017) 6741–6754.
- [33] S.J. Mousavi, N. Nassiri, N. Masoumi, N. Nassiri, M. Majdi-N, S. Farzaneh, A. R. Djalilian, G.A. Peyman, Finite element analysis of blunt foreign body impact on the cornea after PRK and LASIK, *J. Refract. Surg.* 28 (1) (2012) 59–64, <https://doi.org/10.3928/1081597X-20110906-02>.
- [34] G.S. Wilde, H.J. Burd, S.J. Judge, Shear modulus data for the human lens determined from a spinning lens test, *Exp. Eye Res.* 97 (1) (2012) 36–48, <https://doi.org/10.1016/j.exer.2012.01.011>.
- [35] A.L. Sheppard, C.J. Evans, K.D. Singh, J.S. Wolffsohn, M.C. Dunne, L.N. Davies, Three-dimensional magnetic resonance imaging of the phakic crystalline lens during accommodation, *Invest. Ophthalmol. Vis. Sci.* 52 (6) (2011) 3689–3697, <https://doi.org/10.1167/iovs.10-6805>.
- [36] L. Marussich, F. Manns, D. Nankivil, B. Maceo Heilman, Y. Yao, E. Arrieta-Quintero, A. Ho, R. Augusteyn, J.M. Parel, Measurement of crystalline lens volume during accommodation in a lens stretcher, *Invest. Ophthalmol. Vis. Sci.* 56 (8) (2015) 4239–4248, <https://doi.org/10.1167/iovs.15-17050>.
- [37] H.M. Pour, S. Kanapathipillai, K. Zarrabi, F. Manns, A. Ho, Stretch-dependent changes in surface profiles of the human crystalline lens during accommodation: a finite element study, *Clin. Exp. Optom.* 98 (2) (2015) 126–137, <https://doi.org/10.1111/cxo.12263>.
- [38] X. Wang, L.K. Fisher, D. Milea, J.B. Jonas, M.J.A. Girard, Predictions of optic nerve traction forces and peripapillary tissue stresses following horizontal eye movements, *Invest. Ophthalmol. Vis. Sci.* 58 (4) (2017) 2044–2053, <https://doi.org/10.1167/iovs.16-21319>.
- [39] X. Liu, L. Wang, C. Wang, J. Fan, S. Liu, Y. Fan, Prediction of globe rupture caused by primary blast: a finite element analysis, *Comput. Methods Biomech. Biomed. Eng.* 18 (9) (2015) 1024–1029, <https://doi.org/10.1080/10255842.2013.869317>.
- [40] M. Bahrami, M. Hoshino, B. Pierscionek, N. Yagi, J. Regini, K. Uesugi, Optical properties of the lens: an explanation for the zones of discontinuity, *Exp. Eye Res.* 124 (2014) 93–99, <https://doi.org/10.1016/j.exer.2014.05.009>.
- [41] E. Martinez-Enriquez, P. Pérez-Merino, M. Velasco-Ocana, S. Marcos, OCT-based full crystalline lens shape change during accommodation *in vivo*, *Biomed. Opt. Express* 8 (2) (2017) 918–933, <https://doi.org/10.1364/BOE.8.000918>.
- [42] E.A. Hermans, M. Dubbelman, R. Van der Heijde, R.M. Heethaar, Equivalent refractive index of the human lens upon accommodative response, *Optom. Vis. Sci.* 85 (12) (2008) 1179–1184, <https://doi.org/10.1097/OPX.0b013e31818e8d57>.
- [43] M. Dubbelman, G.L. Van Der Heijde, H.A. Weeber, Change in shape of the aging human crystalline lens with accommodation, *Vision Res.* 45 (1) (2005) 117–132, <https://doi.org/10.1016/j.visres.2004.07.032>.
- [44] Z. Liu, B. Wang, X. Xu, C. Wang, A study for accommodating the human crystalline lens by finite element simulation, *Comput. Med. Imag. Graph.* 30 (6–7) (2006) 371–376, <https://doi.org/10.1016/j.compmedimag.2006.09.008>.
- [45] E. Lütjen-Drecoll, P.L. Kaufman, R. Wasielewski, L. Ting-Li, M.A. Croft, Morphology and accommodative function of the vitreous zonule in human and monkey eyes, *Invest. Ophthalmol. Vis. Sci.* 51 (3) (2010) 1554–1564, <https://doi.org/10.1167/iovs.09-4008>.
- [46] M.A. Croft, J. Peterson, C. Smith, J. Kiland, T.M. Nork, J.P. McDonald, A. Katz, S. Hetzel, E. Lütjen-Drecoll, P.L. Kaufman, Accommodative movements of the choroid in the optic nerve head region of human eyes, and their relationship to the lens, *Exp. Eye Res.* 222 (2022), 109124, <https://doi.org/10.1016/j.exer.2022.109124>.
- [47] S. Marcos, S. Ortiz, P. Pérez-Merino, J. Birkenfeld, S. Durán, I. Jiménez-Alfaro, Three-dimensional evaluation of accommodating intraocular lens shift and alignment *in vivo*, *Ophthalmology* 121 (1) (2014) 45–55, <https://doi.org/10.1016/j.jophtha.2013.06.025>.
- [48] L. Shen, W. Yang, D. Li, Z. Wang, W. Chen, Q. Zhao, Y. Li, R. Cui, Q. Liu, Crystalline lens decentration and tilt in eyes with different axial lengths and their associated factors, *Indian J. Ophthalmol.* 71 (3) (2023) 763–767, <https://doi.org/10.4103/ijo.IJO.1054.22>.
- [49] E.A. Hermans, M. Dubbelman, R. Van der Heijde, R.M. Heethaar, Change in the accommodative force on the lens of the human eye with age, *Vision Res.* 48 (1) (2008) 119–126, <https://doi.org/10.1016/j.visres.2007.10.017>.
- [50] D. Nankivil, F. Manns, E. Arrieta-Quintero, N. Ziebarth, D. Borja, A. Amelincx, A. Bernal, A. Ho, J.M. Parel, Effect of anterior zonule transection on the change in lens diameter and power in cynomolgus monkeys during simulated accommodation, *Invest. Ophthalmol. Vis. Sci.* 50 (8) (2009) 4017–4021, <https://doi.org/10.1167/iovs.08-2638>.
- [51] D. Nankivil, B. Maceo Heilman, H. Durkee, F. Manns, K. Ehrmann, S. Kelly, E. Arrieta-Quintero, J.M. Parel, The zonules selectively alter the shape of the lens during accommodation based on the location of their anchorage points, *Invest. Ophthalmol. Vis. Sci.* 56 (3) (2015) 1751–1760, <https://doi.org/10.1167/iovs.14-16082>.
- [52] M. Ruggeri, C. de Freitas, S. Williams, V.M. Hernandez, F. Cabot, N. Yesilirmak, K. Alawa, Y.C. Chang, S.H. Yoo, G. Gregori, J.M. Parel, F. Manns, Quantification of the ciliary muscle and crystalline lens interaction during accommodation with synchronous OCT imaging, *Biomed. Opt. Express* 7 (4) (2016) 1351–1364, <https://doi.org/10.1364/boe.7.001351>.
- [53] I.N. Koshits, O. Svetlova, M.B. Egemberdiev, M.G. Guseva, F.N. Makarov, N.M. R. Roselo Kesada, Theory: morphological and functional features of the structure of the Zonula Lens Fibers as a key executive link in the mechanism of the human eye accommodation, *J. Clin. Res.* 7 (2020) 061–074.
- [54] S.J. Lim, S.J. Kang, H.B. Kim, Y. Kurata, I. Sakabe, D.J. Apple, Analysis of zonular-free zone and lens size in relation to axial length of eye with age, *J. Cataract Refract. Surg.* 24 (3) (1998) 390–396, [https://doi.org/10.1016/S0886-3350\(98\)80329-5](https://doi.org/10.1016/S0886-3350(98)80329-5).
- [55] I. Sakabe, T. Oshika, S.J. Lim, D.J. Apple, Anterior shift of zonular insertion onto the anterior surface of human crystalline lens with age, *Ophthalmology* 105 (2) (1998) 295–299, [https://doi.org/10.1016/S0161-6420\(98\)93172-4](https://doi.org/10.1016/S0161-6420(98)93172-4).
- [56] D.K. Roberts, T.L. Newman, M.F. Roberts, B.A. Teitelbaum, J.E. Winters, Long anterior lens zonules and intraocular pressure, *Invest. Ophthalmol. Vis. Sci.* 59 (5) (2018) 2015–2023, <https://doi.org/10.1167/iovs.17-23705>.
- [57] D.K. Roberts, R. Ayyagari, S.E. Moroi, Possible association between long anterior lens zonules and plateau iris configuration, *J. Glaucoma* 17 (5) (2008) 393–396, <https://doi.org/10.1097/IJG.0b013e31815c3b04>.